Journal of Modern Optics
Vol. 58, Nos. 19–20, 10–20 November 2011, 1781–1787

Taylor & Francis
Taylor & Francis Group

Age-dependent variation of the gradient index profile in human crystalline lenses

Alberto de Castro[a]*, Damian Siedlecki[b], David Borja[c,d], Stephen Uhlhorn[c], Jean-Marie Parel[c,e], Fabrice Manns[c,d] and Susana Marcos[a]

[a]*Instituto de Óptica "Daza de Valdés", Consejo Superior de Investigaciones Científicas, C/ Serrano 121, Madrid 28006, Spain;* [b]*Institute of Physics, Wroclaw University of Technology, Wybrzeze Wyspianskiego 27, 50370 Wroclaw, Poland;* [c]*Ophthalmic Biophysics Center, Bascom Palmer Eye Institute, University of Miami Miller School of Medicine, 1638 NW 10th Avenue, Miami, FL 33136, USA;* [d]*Biomedical Optics and Laser Laboratory, Department of Biomedical Engineering, University of Miami College of Engineering, 1251 Memorial Drive, Coral Gables, FL 33146, USA;* [e]*Vision Cooperative Research Centre, Rupert Myers Building, Sydney, NSW 2052, Australia*

(*Received 30 November 2010; final version received 18 February 2011*)

An investigation was carried out with the aim of reconstructing the gradient index (GRIN) profile of human crystalline lenses *ex-vivo* using optical coherence tomography (OCT) imaging with an optimization technique and to study the dependence of the GRIN profile with age. Cross-sectional images of nine isolated human crystalline lenses with ages ranging from 6 to 72 (post-mortem time 1 to 4 days) were obtained using a custom-made OCT system. Lenses were extracted from whole cadaver globes and placed in a measurement chamber filled with preservation medium (DMEM). Lenses were imaged with the anterior surface up and then flipped over and imaged again, to obtain posterior lens surface profiles both undistorted and distorted by the refraction through the anterior crystalline lens and GRIN. The GRIN distribution of the lens was described with three variables by means of power function, with variables being the nucleus and surface index, and a power coefficient that describes the decay of the refractive index from the nucleus to the surface. An optimization method was used to search for the parameters that produced the best match of the distorted posterior surface. The distorted surface was simulated with accuracy around the resolution of the OCT system (under 15 μm). The reconstructed refractive index values ranged from 1.356 to 1.388 for the surface, and from 1.396 to 1.434 for the nucleus. The power coefficient ranged between 3 and 18. The power coefficient increased significantly with age, at a rate of 0.24 per year. Optical coherence tomography allowed optical, non-invasive measurement of the 2D gradient index profile of the isolated human crystalline lens *ex vivo*. The age-dependent variation of the changes is consistent with previous data using magnetic resonance imaging, and the progressive formation of a refractive index plateau.

Keywords: crystalline lens; gradient index; OCT

1. Introduction

There has been a great interest in understanding of the optical properties of the human crystalline lens over the last few decades. Many of the recent studies aim at gaining knowledge on the contribution of the crystalline lens to the overall retinal image [1,2] mechanism of accommodation [3,4], and its failure in presbyopia [5,6]. A better understanding of the optics of the natural crystalline lens can also help design new intraocular lenses (IOLs), including IOLs which mimic the spherical aberration of the young crystalline lens [7,8], or, a much more challenging goal, IOLs that respond dynamically to accommodation stimuli to restore the accommodative capability of the young crystalline lens [9].

One particularity of the lens is that it continuously grows throughout life. During aging, the crystalline lens undergoes several changes in several physical and biochemical properties, including geometry (thickness, curvatures), mass, volume, stiffness, elasticity and its gradient refractive index [10,11]. Age-dependent changes in the refractive index distribution were postulated by several authors based on the observation that ocular refraction remained practically constant with age, even though the lens shape experienced very significant changes [12–16]. The lens paradox, as this effect was named, hypothesized that the equivalent refractive index should decrease with age in order to compensate for the decrease of the radii of curvature (and therefore increased surface power) of the relaxed crystalline lens with age [17].

Experimental measurements of the gradient index distribution inside the lens and its age dependence have been challenging, and mostly restricted to measurements *in vitro*. For example, Pierscionek [18] measured

*Corresponding author. Email: alberto@io.cfmac.csic.es

ISSN 0950–0340 print/ISSN 1362–3044 online

http://dx.doi.org/10.1080/09500340.2011.565888
http://www.tandfonline.com

the local refractive indices directly using a fiber-optic sensor, and reported no significant variation of the surface index in the anterior and posterior poles with age, although she found that the index at the equator seemed to be lower in younger lenses. Using Purkinje images technique and a very simple GRIN model, Hemenger et al. [15] reported a significantly flatter refractive index near the lens center in older than in younger lenses. Glasser and Campbell [19] measured lens geometry *in vitro* and used a laser ray tracing technique to measure the focal length from which they estimated the equivalent refractive index of the lens. They found no age-dependency of the equivalent refractive index with age. In contrast, Borja et al. [20] reported a biphasic decline of the equivalent refractive index with age. Uhlhorn et al. [21] used, for the first time, optical coherence tomography (OCT) for estimations of the refractive index of human crystalline lenses and reported a decrease in the average (not to be mistaken with equivalent) axial refractive index with age. Magetic resonance imaging (MRI) has been used as a non-destructive method to measure the GRIN distribution of the human crystalline lens, and results have been reported as a function of the age of the donor lenses [22,23]. This technique assumes that the local refractive index is proportional to the water content across the lens. These MRI results suggest that the surface and nucleus refractive index are constant with age, but that there is a flattening of the GRIN profile with age [23]. One limitation of the MRI approach is that the accuracy of the refractive index values depends on the validity and accuracy of the calibration technique. More studies using alternative methods, without the limitations of the MRI technique, are needed to verify the variability of the nucleus and surface refractive index values, and to confirm the changes in the shape of the profile with age.

In a previous work [24] we have presented a new method for the reconstruction of the GRIN distribution of crystalline lenses *in vitro*, based on OCT. The method was demonstrated in isolated porcine lenses, and provided for the first time three-dimensional (3D) reconstructions of a complex crystalline lens GRIN distribution. The method is based on the acquisition of OCT images of the lens (pairs of images with the anterior surface up and down), and an optimization routine based on a genetic algorithm. We have also shown that the presence of the GRIN contributes significantly to the distortion of the posterior lens surface seen through the anterior surface [25]. In the present study we have applied the GRIN reconstruction method to the two-dimensional reconstruction of the GRIN from OCT images of human cadaver lenses of different ages.

2. Methods

2.1. Human lens samples

Human eyes were obtained from the Florida Lions Eye Bank and used in compliance with the guidelines of the Declaration of Helsinki for research involving the use of human tissue. Experiments were performed on nine lenses from nine different donor eyes within 1 to 4 days post-mortem. The donor age ranged from 6 to 72 years (average 44 ± 20 years). The donor globes arrived in sealed vials, wrapped in gauze soaked with BSS. Upon receipt, the vials were stored in a fridge at 4°C. Before the experiment, the vials were removed from the fridge and the lens was carefully extracted and immersed in preservation medium (DMEM/F-12, D8437, Sigma, St. Louis, MO) at 25°C, using a protocol that has been published previously [26]. During measurements, the lens rested at the bottom of a cuvette on a soft rubber o-ring (Buna-N, Small Parts Inc, Miami, FL), which prevents any contact of the lens surface with the chamber wall [21]. All measurements were performed within an hour after the lens was extracted from the eye. Lenses that were swollen or damaged, as determined from the OCT image and the methods described in Augusteyn et al. [26], were excluded from the study.

2.2. OCT imaging

Lenses were imaged with a custom-built time domain OCT system in two positions, with the anterior surface of the lens facing the OCT beam, and then in the reversed orientation (posterior surface lens up). The lens was carefully flipped and re-aligned with a surgical spoon and special care was taken to ensure that the OCT cross-sectional images were obtained on the same meridians for the two orientations of the lens, first visually and then by using features in preliminary OCT images as a guide. In practice, however, small differences in the alignment, which increase the variability of the results, are always expected.

The OCT system used to image the lenses has 8 μm axial resolution, 60 μm lateral resolution, and a 10 mm optical scan length, corresponding to approximately 7.5 mm imaging depth in tissue. A telecentric beam delivery system produces a flat scan field with a maximum lateral scan length of 20 mm. The lens was centered using continuous real-time display of the central A-scan and tilt ant tip adjusted using real-time B-scan images. Each cross-sectional OCT image consists of 500 A-lines acquired over a 10 mm lateral scan length with 5000 points per A-line.

2.3. Image processing

An edge-detection routine developed in MATLAB (MathWorks, Natick MA) was used to detect the position of the intensity peaks corresponding to the anterior and posterior surfaces of the lens on each A-scan of the uncorrected OCT image. Any residual tilt was corrected using a procedure that has been described before [27,28].

The optical path difference (OPD) for each ray was calculated as the vertical distances between anterior and posterior lens surfaces in an uncorrected (distorted) OCT image. The actual shape of the lens was obtained from the undistorted images of the anterior and posterior surfaces. The segmented surfaces were fitted by conics. The true physical thickness of each lens was calculated from the distortion of the cuvette holding the lens during the measurements [21]. The average refractive index along the central axis was calculated dividing the optical thickness by the geometrical thickness of the lens. This calculation produces the average group refractive index for the OCT wavelength (825 ± 25 nm). The group refractive index was converted to a phase refractive index for mononochromatic light at 825 nm. The phase refractive index at 589 nm was then calculated using lens dispersion data from the literature [29] in a similar way as reported by Uhlhorn et al. [21].

2.4. GRIN reconstruction algorithm

The GRIN profile of the lenses was estimated using an optimization method that we have presented in a previous publication, and demonstrated in porcine crystalline lenses [24]. In the previous study the method was applied on 3D OCT images of a porcine lens, while here it is applied to two-dimensional (2D) OCT images of human lenses. A merit function was built based on the difference between the experimental OPD data and the estimated OPD of each ray through a GRIN model (i.e. a genetic/Nelder–Mead algorithm searched for the best GRIN that matched the experimental optical path differences, the minimum of the merit function). The variables in the minimization procedure were those of the GRIN model.

Although the reconstruction was performed for several pupil diameters, the best results (lower values in the merit function) were found for 4 mm pupil diameters, and the reconstructed GRIN parameters are given for this pupil diameter.

2.5. GRIN model

A three-variable GRIN model was used in the reconstruction [30]. The center of the lens was set in the meridional plane, at 0.41 times the thickness of the lens [10]. The GRIN was described by means of a power coefficient from the nucleus (with a refractive index n_N) to the surface (with refractive index n_S):

$$n(\rho,\theta) = n_N - \Delta n\left(\frac{\rho}{\rho_S(\theta)}\right)^p, \tag{1}$$

where Δn is the difference between nucleus and surface refractive indices, ρ_S is the distance from the center of the lens to the surface at angle θ, and p is the power coefficient of the GRIN.

A similar model (with additional variables to account for meridional variations in the refractive index) had been successfully used to reconstruct the GRIN 3D distribution in porcine lenses. The power coefficient allows the description of highly distributed refractive index (low exponents) as expected in young lenses, as well as a constant plateau and rapid decline of the refractive index toward the surface (high exponents) as expected in old lenses. The only constraint used in the search algorithm was a penalty if the surface refractive index was higher than the nucleus index.

3. Results

3.1. Lens shape and thickness

Anterior and posterior lens surfaces of the lenses were fitted by conics over a 6 mm area. Fitting errors were in all cases in the order of the OCT resolution. Figure 1 shows the values of anterior and posterior radii of curvature and thickness as a function of age. Lenses steepened with age until at least 50 years.

3.2. Average refractive index

The average refractive index is the mean value of the GRIN profile along the optical axis of the lens. Figure 2 shows the average phase refractive index as a function of age at 589 nm. As reported previously in the literature [21], there is no clear age-related trend, and there is a wide range of average index values (1.392 to 1.425) for the 9 lenses measured in this study. The two extreme values for the adult eyes (at 31 and 49 years) could be caused by variability in the measurement due to positioning errors.

3.3. Gradient index distribution

Table 1 shows the GRIN model parameters obtained in the reconstruction, and Figure 3 the age-dependence of the three parameters: nucleus and surface indices (Figure 3(*a*)) and power coefficient (Figure 3(*b*)).

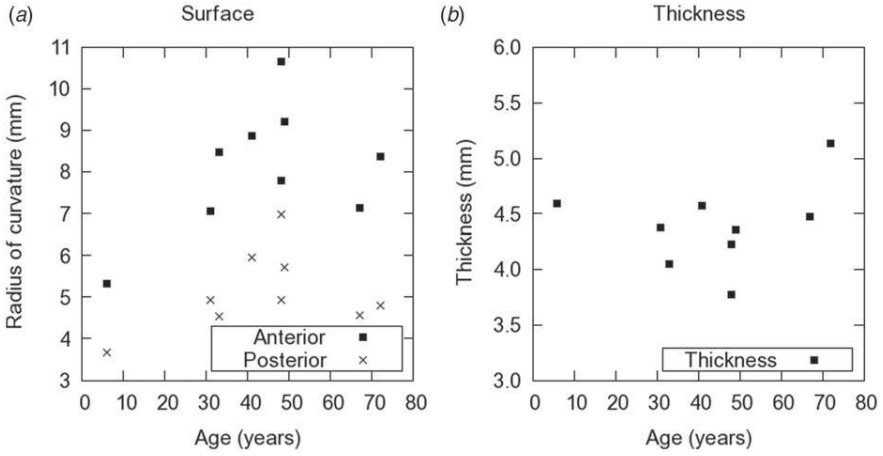

Figure 1. (*a*) Radii of curvature of the anterior and posterior surfaces of the lenses used in this study. (*b*) Thickness calculated from the OCT images.

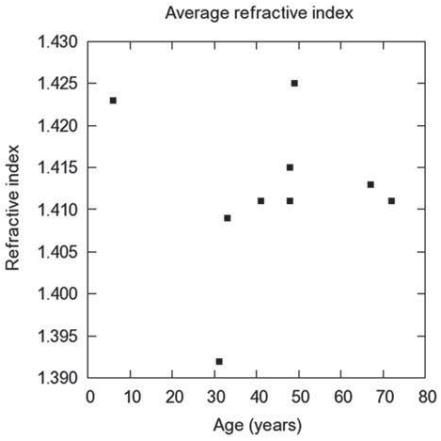

Figure 2. Average phase refractive index at 589 nm as a function of age.

Table 1. Values of average index and GRIN parameters: surface and nucleus refractive index and power coefficient for the set of lenses imaged in this study. An asterisk in the age column indicates that a secondary minimum was taken as solution. All refractive index values correspond to phase refractive index calculated at 589 nm.

Age	Average	GRIN results		
(years)	(phase 598 nm)	Surface	Nucleus	Exp decay
6	1.423	1.386	1.434	3.2
*31	1.392	1.362	1.399	3.6
*33	1.409	1.388	1.414	7.6
*41	1.411	1.387	1.418	4.4
48	1.411	1.351	1.412	11.9
48	1.415	1.356	1.418	13.6
*49	1.425	1.382	1.432	6.5
67	1.413	1.365	1.412	17.7
72	1.411	1.376	1.413	16.7

The only systematic variation with age was found for the power coefficient. The goodness of the reconstruction (comparison of the experimental distorted posterior lens surface and the simulated from the reconstructed GRIN) was less than 15 μm in all cases.

In four lenses (ages 31, 33, 41 and 49) the lowest RMS was found with a homogeneous index (similar nucleus and surface indices). A study of the space of solutions revealed another pair of values that represented the experimental OPDs with high accuracy (RMS = 6 ± 5 μm). For these lenses, another realization of the local search algorithm produced a local minimum, which was taken as the solution of the optimization problem.

There was no statistically significant change with age in the refractive index of surface and nucleus ($p = 0.37$ and 0.39, respectively). Average refractive index values in surface and nucleus was found to be 1.373 ± 0.014 and 1.417 ± 0.011. The power coefficient increased steadily with age and significantly ($p = 0.039$), with a rate given by 0.24 ± 0.05 ($r = 0.847$) per year. All values correspond to the phase index at 589 nm.

Figure 4 shows raw OCT images and the 2D representations of the reconstructed GRIN in the nine lenses of the study.

4. Discussion

We have shown that OCT imaging allows high-resolution imaging of the crystalline lens surfaces as well as reconstruction of the GRIN distribution of the isolated lens. In a small group of eyes, we found age-dependent variation of the lens shape, and changes in the shape of the GRIN profile.

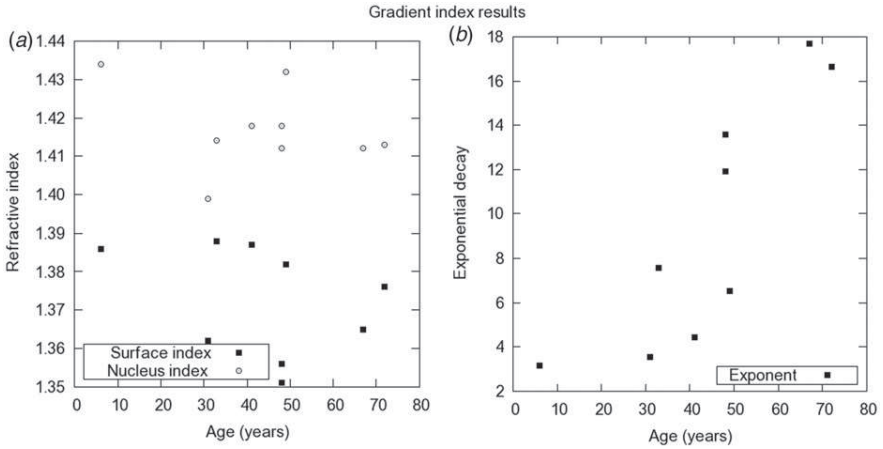

Figure 3. Nucleus and surface refractive indices (*a*) and power coefficient (*b*). The refractive index values correspond to the phase refractive index at 589 nm.

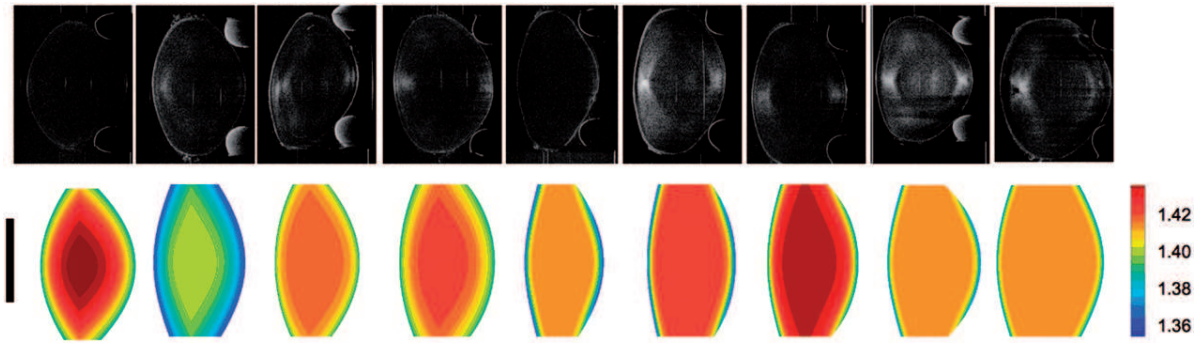

Figure 4. Two-dimensional OCT image (upper row) and reconstructed GRIN distribution (lower row) of the nine lenses of the study. Data of the central 4 mm pupil were used, the vertical black bar indicates the area reconstructed. (The color version of this figure is included in the online version of the journal.)

We found similar changes in the radii of curvature to those reported by Borja et al. [20] in isolated lenses using shadowphotography. The changes are more prominent in the anterior surface, as previously reported to occur *in vivo* as a function of age and as a function of accommodation [4,31,32]. A remarkable feature is the biphasic pattern of the variation of the lens radii with age [20].

The surface and nuclear refractive indices were found to be constant with age. However, the values suffered from a relatively large scatter. A larger number of samples is required to confirm with statistical certainty if these indices change with age. The lack of systematic variation of the surface and nucleus indices with age had been previously reported using destructive methods [18] and with the MRI approach [23] on a larger population. The shape of the GRIN profile varied significantly with age, with a more distributed index in the young lens, and an increase of the central plateau with increasing age, confirming results obtained from a Purkinje method [15] and MRI [22,23]. The average refractive index does not change systematically with age, in agreement with previously published results [21]. The range of refractive indices (1.392 to 1.425) is similar to previous reports (1.316 to 1.416), and the scattering of the data is large in all studies. The reconstructed surface and nucleus indices of refraction also show a large intersubject variability. The variability of the surface and nucleus indices is probably not the reflection of the true biological variability, but caused by measurement uncertainties. A precision of ± 0.01 in the refractive index correspond to a relative error of less than 1%. In general, the lens refractive index is derived indirectly from several independent measurements, each with its own sources of error. Small measurement errors can produce significant variations of the refractive index. In our study, the refractive index is calculated from two

separate images of the crystalline lens. The extreme values of two of the adult lenses could be due to small positioning errors between the two measurements (see below). Overall, our reconstructed indices (1.351 to 1.388 for the surface refractive index and 1.399 to 1.434 for the nucleus refractive index) are in agreement with those from Jones et al. [23] using MRI (1.36 and 1.38 for the surface refractive index and 1.395 to 1.430 for the nucleus refractive index).

The only parameter that is found to change systematically with age is the power coefficient of the GRIN model. Some studies in the literature describe the progressive development of a central refractive index plateau area in the lens with aging [11,23]. The three-variable model can account for a systematic variation of the profile (low power coefficients) or the presence of a plateau (high power coefficients), without requiring a highly complex GRIN model definition. We found that the power coefficient increases steadily with age. This is consistent with a monotonic variation of the profiles in young lenses, and a relatively flat profile, with a steep decrease of the index near the surface in old lenses. These results are in accordance with previous literature using MRI of the change of the GRIN structure in crystalline lenses with age [23].

The use of OCT imaging to reconstruct GRIN in the human lens is novel. We had theoretically suggested that optical path differences from OCT contained information of the GRIN distribution in 2004 [33]. The first experimental application of OCT to retrieve GRIN was performed in the fish lens (using a simple spherical lens and spherical GRIN model) by Verma et al. in 2007 [34]. We have recently presented a new GRIN reconstruction method from 3D OCT images in a porcine lens [24]. In humans, we have recently reported the relevance of the distortion produced by GRIN in the visualization of the posterior lens surface [25]. The difference between the distorted and undistorted lens shape is a key factor in the reconstruction. The OCT technique provides high resolution in surface shape measurements (in comparison with shadowphotography or Scheimpflug) and GRIN estimates (in comparison with MRI). The precision of the GRIN reconstruction technique is mainly limited by experimental errors. Lens surface elevation is limited by the resolution of the OCT system (around 10 μm in our system) and the centration of the lens. Tilt is corrected in the images but residual tilt, and particularly a decentration of the lens (i.e. A-scan not passing through the apex of the lens) will result in an underestimation of the thicknesses and overestimation of the radii of curvature. Also, although special care was taken to ensure that, when flipping the lens over, the meridian under measurement remained unchanged, errors may arise due to decentration or rotation. If rotated, astigmatism in the surfaces or possible assymetries in the GRIN distribution will introduce an error in the measurements. While we believe that these effects are not significantly affecting the overall findings, they increase the variability. In particular, potential trends for variations in the surface and nucleus index can be confirmed by increasing the sample size. Also, some of the errors can be minimized by extending the method to 3D images of the lens. Future 3D reconstruction will also make it possible to take into account the possible astigmatism of the lens surfaces and meridional variations in the GRIN profile.

Acknowledgements

The authors are grateful to Bianca Maceo and Raksha Urs for assistance with data processing. The study was supported in part by National Eye Institute Grants 2R01EY14225, 5F31EY15395 (NRSA Individual Predoctoral Fellowship, Borja), P30EY14801 (Center Grant); the Florida Lions Eye Bank; the Henri and Flore Lesieur Foundation (JMP); an unrestricted grant from Research to Prevent Blindness and the Vision Cooperative Research Centre, Sydney, New South Wales, Australia, supported by the Australian Federal Government through the Cooperative Research Centres Programme; and Grants FIS2008-02065 (Ministerio de Ciencia e Innovación, Spain), EURYI-05-102-ES (EURHORCs-ESF), CSIC I3P Predoctoral and JAE-DOC Postdoctoral Programs.

References

[1] Smith, G.; Cox, M.J.; Calver, R.; Garner, L. *Vision Res.* **2001,** *41,* 235–243.
[2] Artal, P.; Berrio, E.; Guirao, A.; Piers, P. *J. Opt. Soc. Am. A* **2002,** *19,* 137–143.
[3] Rosales, P.; Dubbelman, M.; Marcos, S.; van Der Heijde, R.G.L. *J. Vision* **2006,** *6,* 1057–1067.
[4] Rosales, P.; Wendt, M.; Marcos, S.; Glasser, A. *J. Vision* **2008,** *8,* 1–12.
[5] Croft, M.A.; Glasser, A.; Kaufman, P.L. *Int. Ophthalmol. Clin.* **2001,** *41,* 33–46.
[6] Charman, W.N. *Clin. Exp. Optom.* **2008,** *91,* 207–225.
[7] Holladay, J.T.; Piers, P.A.; Koranyi, G.; van Der Mooren, M.; Norrby, S. *J. Refract. Surg.* **2002,** *18,* 683–691.
[8] Marcos, S.; Barbero, S.; Jiménez-Alfaro, I. *J. Cataract Refract. Surg.* **2005,** *21,* 223–235.
[9] Glasser, A. *Clin. Exp. Optom.* **2008,** *91,* 279–295.
[10] Rosen, A.M.; Denham, D.B.; Fernandez, V.; Borja, D.; Ho, A.; Manns, F.; Parel, J.-M.; Augusteyn, R.C. *Vision Res.* **2006,** *46,* 1002–1009.
[11] Augusteyn, R.C.; Jones, C.E.; Pope, J.M. *Clin. Exp. Optom.* **2008,** *91,* 296–301.
[12] Koretz, J.F.; Handelman, G.H. *Int. J. Math. Modelling* **1986,** *7,* 1003–1014.
[13] Pierscionek, B.K. *Clin. Exp. Optom.* **1990,** *73,* 23–30.

[14] Smith, G.; Atchison, D.A.; Pierscionek, B.K. *J. Opt. Soc. Am. A* **1992,** *9,* 2111–2117.
[15] Hemenger, R.P.; Garner, L.; Ooi, C.S. *Invest. Ophthalmol. Vis. Sci.* **1995,** *36,* 703–707.
[16] Garner, L.; Ooi, C.S.; Smith, G. *Clin. Exp. Optom.* **1998,** *81,* 145–150.
[17] Koretz, J.F.; Cook, C.; Kaufman, P.L. *Invest. Ophthalmol. Vis. Sci.* **1997,** *38,* 569–578.
[18] Pierscionek, B.K. *Exp. Eye Res.* **1997,** *64,* 887–893.
[19] Glasser, A.; Campbell, M.C.W. *Vision Res.* **1999,** *39,* 1991–2015.
[20] Borja, D.; Manns, F.; Ho, A.; Ziebarth, N.; Rosen, A.M.; Jain, R.; Amelinckx, A.; Arrieta, E.; Augusteyn, R.C.; Parel, J.-M. *Invest. Ophthalmol. Vis. Sci.* **2008,** *49,* 2541–2548.
[21] Uhlhorn, S.; Borja, D.; Manns, F.; Parel, J.-M. *Vision Res.* **2008,** *48,* 2732–2738.
[22] Moffat, B.A.; Atchison, D.A.; Pope, J.M. *Vision Res.* **2002,** *42,* 1683–1693.
[23] Jones, C.E.; Atchison, D.A.; Meder, R.; Pope, J.M. *Vision Res.* **2005,** *45,* 2352–2366.
[24] de Castro, A.; Ortiz, S.; Gambra, E.; Siedlecki, D.; Marcos, S. *Opt. Express* **2010,** *18,* 21905–21917.
[25] Borja, D.; Siedlecki, D.; de Castro, A.; Uhlhorn, S.; Ortiz, S.; Arrieta, E.; Parel, J.-M.; Marcos, S.; Manns, F. *Biomed. Opt. Express* **2010,** *1,* 1331–1340.
[26] Augusteyn, R.C.; Rosen, A.M.; Borja, D.; Ziebarth, N.M.; Parel, J.-M. *Mol. Vision* **2006,** *12,* 740–747.
[27] Urs, R.; Manns, F.; Ho, A.; Borja, D.; Amelinckx, A.; Smith, J.; Jain, R.; Augusteyn, R.; Parel, J.-M. *Vision Res.* **2009,** *49,* 74–83.
[28] Urs, R.; Ho, A.; Manns, F.; Parel, J.-M. *Vision Res.* **2010,** *50,* 1041–1047.
[29] Atchison, D.A.; Smith, G. *J. Opt. Soc. Am. A* **2005,** *22,* 29–37.
[30] Manns, F.; Ho, A.; Borja, D.; Parel, J.-M. *Invest. Ophthalmol. Vis. Sci.* **2010,** *51,* E–abstract 789.
[31] Dubbelman, M.; van Der Heijde, R.G.L.; Weeber, H.A. *Vision Res.* **2005,** *45,* 117–132.
[32] Koretz, J.F.; Cook, C.A.; Kaufman, P.L. *J. Opt. Soc. Am. A* **2002,** *19,* 144–151.
[33] Ortiz, S.; Barbero, S.; Marcos, S. *Invest. Ophthalmol. Vis. Sci.* **2004,** *45,* E-abstract 2781.
[34] Verma, Y.; Rao, K.D.; Suresh, M.K.; Patel, H.S.; Gupta, P.K. *Appl. Phys. B* **2007,** *87,* 607–610.